

# Effect of Interface Modification on the Performances of TiO<sub>2</sub>-based Perovskite Solar Cells

Wenmei Gu, Tianwei Li, Rui Zha, Jincheng Zhou

*School of Material Science and Engineering, Shenyang Architecture University, Shenyang, 110168, China*

**Abstract:** TiO<sub>2</sub> was used as the basis of Electron Transport Layers (ETLs), and the interface modification of ETLs was carried out using sixteen alkyl three methyl bromide (C<sub>16</sub>H<sub>33</sub>(CH<sub>3</sub>)<sub>3</sub>NBr, CTAB), which plays the roles of filling pores and passivating surface defects. The effects of the doping concentration of 0.005 mol/L, 0.010 mol/L, and 0.015 mol/L CTAB solution on the device efficiency were investigated separately, and the mechanism of the effects of different concentrations was explored. The surface morphology and the photoelectric properties of the samples were systematically investigated by SEM, EIS, J-V, and transmittance tests.

**Keywords:** perovskite solar cell; electron transport layer; CTAB; interface modification

## 1. Introduction

Organic-inorganic hybridized perovskites have attracted much attention due to their excellent photovoltaic properties and have been used to fabricate low-cost and high-efficiency solar cells [1-3]. TiO<sub>2</sub>, as the earliest electron transport material applied in perovskite solar cells, is widely used in perovskite solar cells (PSCs) [4], which is characterized by high thermal stability, excellent photovoltaic properties, and low cost. Solar cells (PSCs) [4], and currently the planar-structured perovskite solar cells based on TiO<sub>2</sub> electron transport layers (ETLs) have achieved a high efficiency of 24.8% [5].

Nam-Gyu Park [6] et al. spin-coated a very thin layer of MgO on the surface of planar-structured TiO<sub>2</sub> by sol-gel method, which was able to passivate the TiO<sub>2</sub> surface defect state density, thus reducing the carrier recombination at the TiO<sub>2</sub>/CH<sub>3</sub>NH<sub>3</sub>PbI<sub>2</sub> interface, increasing the open-circuit voltage and fill factor of the cell, which in turn improved the cell performance. Hanyin Li and others [7] modified the ZnO dense layer with 3-aminopropionic acid to fabricate planar perovskite solar cells. After interface modification, the perovskite layer formed a more uniform and dense morphology on the ZnO surface, and the absorption was enhanced to some extent. Additionally, the dipole effect made the energy levels of ZnO and the perovskite more compatible, and the small molecule enhanced the electron coupling between the ZnO layer and the perovskite layer. Combining these factors, the photovoltaic conversion efficiency of the cell was increased to 15.7%. Wang and his team have achieved a maximum PCE of 19.03% by using C60-SAM for passivation on TiO<sub>2</sub> ETLs. C60-SAM effectively passivates the surface of metal oxides and promotes charge transfer at the SnO<sub>2</sub> ETLs/perovskite interface [8].

Chen and his team utilized a chlorinated imidazole ionic liquid, 4-imidazole acetic acid hydrochloride (ImAcHCl), to modify the SnO<sub>2</sub> ETLs. The lone pair electrons on the nitrogen atoms of the imidazole group in ImAcHCl were expected to passivate the defects in the perovskite layer, thereby improving the Voc (open-circuit voltage) of SnO<sub>2</sub>. As a result, the Voc of the device was increased from 1.084 V before modification to 1.143 V, and the PCE (power conversion efficiency) was enhanced from 19.5% to 21% [9].

The experiments were carried out using TiO<sub>2</sub> as the basis of ETLs, and the ETLs were modified using CTAB, the structure of which is shown in Fig. 1, which is chemically stable, resistant to strong acids and bases, resistant to light and heat, and possesses excellent permeation and softening characteristics [10]. This substance was introduced into the ETLs as a surfactant, and the effects of the doping concentrations of 0.005 mol/L, 0.010 mol/L, and 0.015 mol/L CTAB solutions on the device efficiency were investigated separately, and the mechanism of the effects of different concentrations was systematically investigated by the SEM, EIS, J-V, and UV-vis tests.

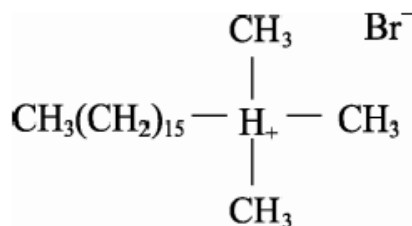


Figure 1: Structure of CTAB

## 2. Experimental process

### 2.1 Preparation of raw materials

- Titanium butoxide ( $\text{Ti}(\text{OC}_4\text{H}_9)_4$ , 99.0% AR, Zhiyuan (Tianjin) Chemical Reagent Co., Ltd.); Cetyltrimethylammonium bromide (CTAB, AR analytical pure, Tianjin Damao Chemical Reagent Factory); Lead iodide ( $\text{PbI}_2$ , 99%, Jieshikai); Iodomethylammonium iodide ( $\text{CH}_3\text{NH}_3\text{I}$ , (MAI), 99.5%, Jieshikai); 2, 2',7,7' -tetrakis[N,N-bis(4-methoxyphenyl)amino]-9,9'-spirobifluorene (Spiro-OMeTAD, 99.5%, Jetstream); Bis(trifluoromethanesulfonyl)imide (Li-TFSI, 99% AR, Jetstream); 4-tert-butylpyridine (TBP,  $\text{C}_9\text{H}_{13}\text{N}$ , 96% AR, Aladdin); Dimethyl sulfoxide (DMSO,  $\text{C}_2\text{H}_6\text{SO}$ , 99.8% AR, Jiuding Chemical); N, N-dimethyl-Formamide (DMF,  $\text{C}_3\text{H}_7\text{NO}$ , 99.5% AR, Zhiyuan (Tianjin) Chemical Reagent Co., Ltd.); Chlorobenzene ( $\text{C}_6\text{H}_5\text{Cl}$ , 99% AR, Jieshikai); Acetonitrile ( $\text{C}_2\text{H}_3\text{N}$ , 99.5% AR, Kermel); Silver (Ag, 99.999%, Zhongnuo New Material (Beijing) Co.)

### 2.2 Device preparation

#### (1) Preparation of $\text{TiO}_2$ solution

Take 25 ml of ethanol solution, add an appropriate amount of acetic acid, and stir for 30 min. During the stirring process, slowly add 1.5 ml of acetylacetone and 3 ml of butyl titanate, and continue stirring for 4 hours to ensure thorough mixing. After a period of standing, a clear yellow solution will be obtained.

#### (2) Equipping of CTAB sols

Take 10 ml of anhydrous ethanol and add 0.18218 g, 0.36436 g, 0.54654 g of CTAB powder, configured into a molar concentration of 0.005 mol/L, 0.010 mol/L, 0.015 mol/L, respectively, stirred for 2h at room temperature.

#### (3) Preparation of perovskite precursor

Dissolve 0.5562 g of  $\text{PbI}_2$  and 0.1980 g of MAI in 1 mL of DMF solution and stir until fully dissolved, let stand for 12h and then ready for use.

#### (4) Preparation of cavity transport material

73.4 mg of Spiro-OMeTAD was dissolved in 1 mL of chlorobenzene solution and stirred for 1 h. 27.5  $\mu\text{L}$  of 4-tert-butylpyridine (TBP) and 18.8  $\mu\text{L}$  of lithium salt acetonitrile solution (260 mg of Li-TFSI was dissolved in 500  $\mu\text{L}$  of acetonitrile) were added, and stirred for 2 h. The solution was then stirred for 1 h. The solution was then stirred for 2 h.

#### (5) Preparation of battery devices

The ITO conductive glass was washed several times with deionized water and anhydrous ethanol and dried. Using ultrasonic precision sprayer, set the instrument parameters as substrate temperature 200 °C, spraying flow rate of 30  $\mu\text{L}/\text{min}$ , spraying air pressure 0.010MPa, spraying power 2.5W, spraying on the ITO glass substrate to prepare  $\text{TiO}_2$  films with different doping contents, the prepared  $\text{TiO}_2$  film was heated on the heating plate at 350 °C for 1 h. Take a certain amount of CTAB solution drops to the  $\text{TiO}_2$  film, spin coating parameters at 2000rpm 30s, after the end, the film was placed on the heating plate at 180 °C and heated for 60h. On the  $\text{TiO}_2$  film with spin coating parameter of 2000 rpm for 30s, after that the film was placed on a heating plate at 180 °C for 60min and cooled to room temperature after heating. Next, the different  $\text{TiO}_2$  films prepared were transferred to a glove box for

the perovskite layer preparation. The perovskite layer was obtained by taking 80  $\mu\text{L}$  of perovskite precursor solution with a pipette gun at 3500 rpm for 50 s, adding 80  $\mu\text{L}$  of anti-solvent chlorobenzene at the 7th s, and then annealing for 30 min on a 100  $^{\circ}\text{C}$  heating plate. After cooling, 80  $\mu\text{L}$  of hole transport material solution was added dropped on the perovskite surface, and the hole transport layer was spin-coated at 3000 rpm for 20 s. The surface of the perovskite layer was coated by magnetron sputtering. The Ag electrode was obtained by magnetron sputtering coating, and the process parameters were set as sputtering power of 60 W, sputtering air pressure of  $1.2 \times 10^{-3}$  Pa, and sputtering time of 60 s. The Ag electrode was deposited on the surface of the hole layer.

### 3. Results and Discussion

Figure 2 shows the SEM images of  $\text{TiO}_2/\text{CTAB}$  films at different concentrations. As can be seen from the figure, when the concentration is 0.005 mol/L, the surface is flat and smooth, the surface of  $\text{TiO}_2$  film is completely covered by the filling, and the CTAB is fully filled in the gaps of  $\text{TiO}_2$ ; when the concentration is 0.010 mol/L, the surface is flat and smooth, but there are agglomerated CTAB particles, with smaller agglomeration sizes, and the dispersion is more extensive; when the concentration is 0.015 mol/L, the surface flatness rises compared with the unspin-coated  $\text{TiO}_2$  film, but the filling of CTAB decreases. When the concentration is 0.015 mol/L, the surface flatness increases compared with the unspin-coated  $\text{TiO}_2$  film, but the filling of CTAB decreases, the grain boundary of the original  $\text{TiO}_2$  film can be seen, and the size of the agglomerated CTAB particles increases, and the agglomerated particles are more concentrated.

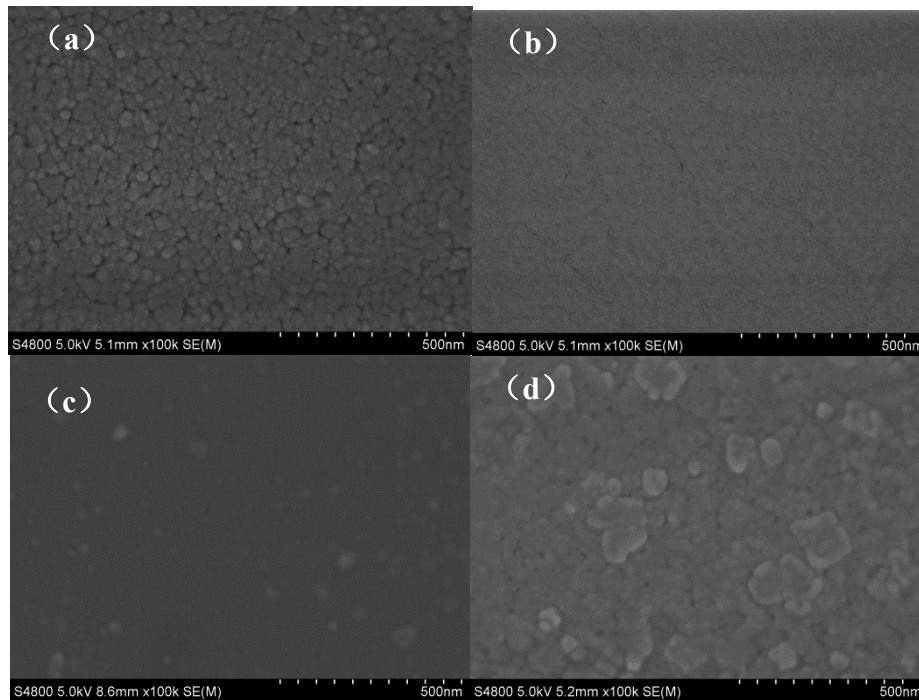


Figure 2: Surface SEM images of samples doped CTAB at different concentrations: (a) without CTAB, (b) 0.005 mol/L, (c) 0.010 mol/L and (d) 0.015 mol/L

Figure 2 shows the SEM images of  $\text{TiO}_2/\text{CTAB}$  films at different concentrations. As can be seen from the figure, when the concentration is 0.005 mol/L, the surface is flat and smooth, the surface of  $\text{TiO}_2$  film is completely covered by the filling, and the CTAB is fully filled in the gaps of  $\text{TiO}_2$ ; when the concentration is 0.010 mol/L, the surface is flat and smooth, but there are agglomerated CTAB particles, with smaller agglomeration sizes, and the dispersion is more extensive; when the concentration is 0.015 mol/L, the surface flatness rises compared with the unspin-coated  $\text{TiO}_2$  film, but the filling of CTAB decreases. When the concentration is 0.015 mol/L, the surface flatness increases compared with the unspin-coated  $\text{TiO}_2$  film, but the filling of CTAB decreases, the grain boundary of the original  $\text{TiO}_2$  film can be seen, and the size of the agglomerated CTAB particles increases, and the agglomerated particles are more concentrated.

The wettability of a material's surface is determined by the nature and buildup of atoms or groups of atoms on the surface, independent of the nature and arrangement of atoms or molecules within. The

wettability of a material surface is determined by two factors: chemical composition and microstructure. In order to check whether different concentrations of CTAB affect the wettability of the TiO<sub>2</sub> sol surface, a contact angle test was carried out and the results are shown in Figure 3 below. Figure (a) shows the wetting angle of unspin-coated CTAB and (b)-(d) shows the wetting angle of spin-coated CTAB with different concentrations. As can be seen from the figures, the wetting angles were  $\theta = 4.164^\circ$ ,  $\theta = 3.904^\circ$ ,  $\theta = 4.672^\circ$  and  $\theta = 13.303^\circ$ . The contact angle increases with increasing concentration. When the concentration was low, the TiO<sub>2</sub>/CTAB surface was dense and uniform, and the contact angle was small; when the concentration was 0.015 mol/L, the modification of TiO<sub>2</sub> surface by CTAB was poor, and agglomeration occurred on the surface, which instead increased the contact angle. The decrease of contact angle is favorable to the deposition of perovskite and improve its film quality.

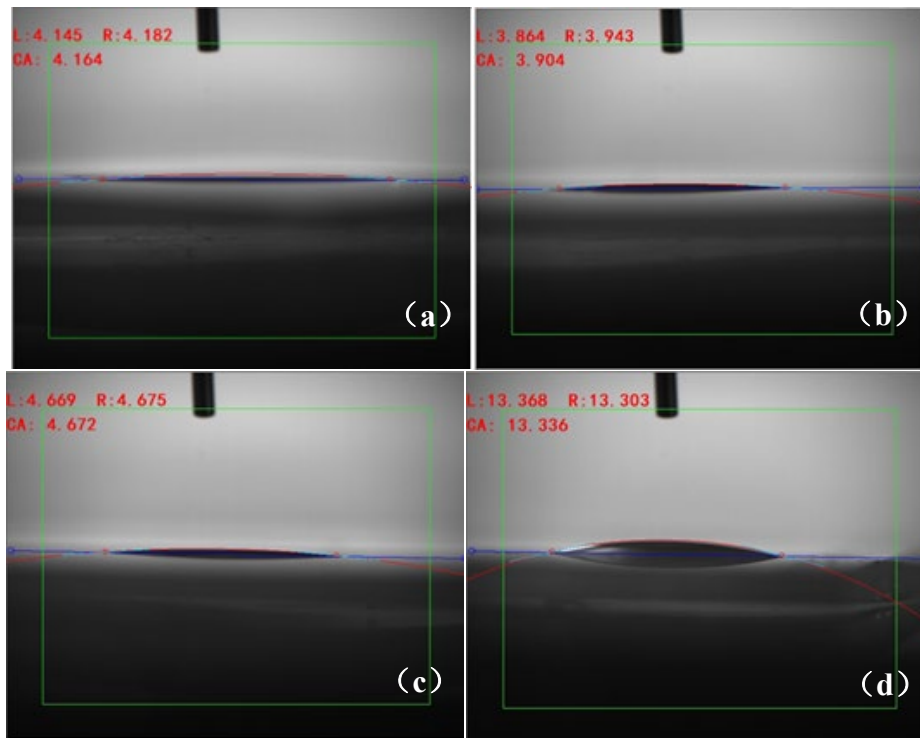


Figure 3: Contact angles of the samples doped with CTAB: (a) without CTAB, (b) 0.005 mol/L, (c) 0.010 mol/L and (d) 0.015 mol/L

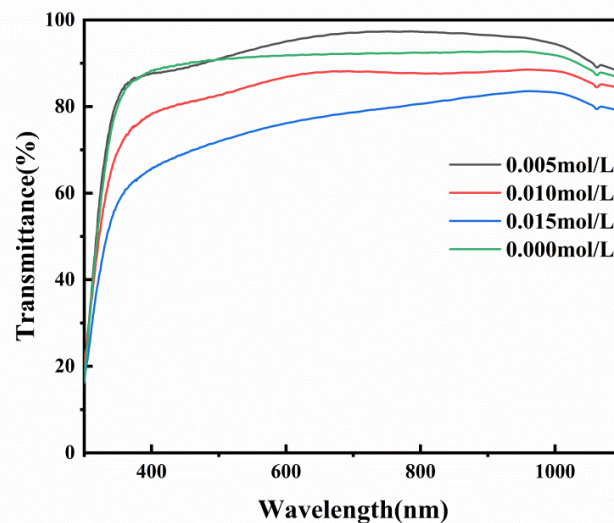


Figure 4: Transmittance curves of the samples with different CTAB concentrations

The transmittance of TiO<sub>2</sub>/CTAB films at different concentrations was tested as shown in Fig. 4. As can be seen from the figure, but the doping concentration of 0.005 mol/L transmittance increased, but the higher concentration of 0.010mol/L and 0.015 mol/L, compared with the undoped TiO<sub>2</sub>, the film transmittance decreased, which corresponds to Figure 2.

Table 1: Photoelectric parameters of the TiO<sub>2</sub> ETLs modified with different concentrations of CTAB

Concentration of CTAB (mol/L)	Voc(V)	Jsc(Ma/cm <sup>2</sup> )	FF(%)	PCE(%)
Without	0.36	3.17	61.59	0.70
0.005mol/L	0.37	3.01	60.32	0.68
0.010mol/L	0.34	3.01	62.84	0.66
0.015mol/L	0.35	2.88	62.31	0.63

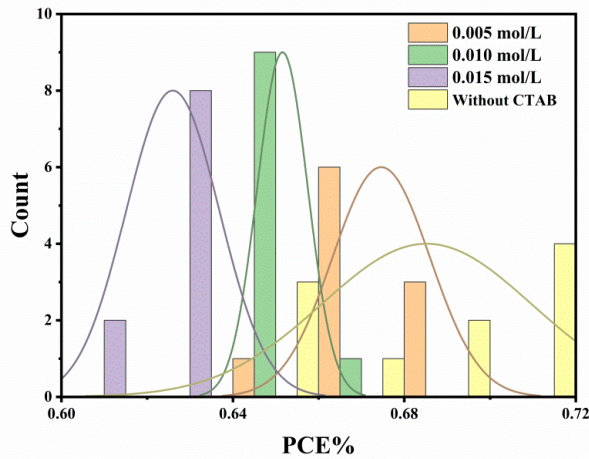


Figure 5: Histogram of PCE distribution of cell devices at different concentrations

The photovoltaic performance parameters of the PSCs cells prepared by using TiO<sub>2</sub> films doped with different concentrations of CTAB as ETLs are shown in Table 1. Although the photovoltaic performance decreases compared with that of the unmodified ones, it can be seen that the interface modification plays a certain role in the passivation of the interfacial defects and filling of the surface porosity in conjunction with the SEM images. In order to ensure the objectivity of the results, 10 devices with different modification concentrations were assembled, and their photoelectric conversion efficiencies (PCEs) were collected, and the histograms of the statistical distributions were plotted as shown in Fig. 5. As shown in Figure5, the PCE of the modified cell devices is relatively concentrated and the stability is improved. Therefore, the effect of CTAB modified TiO<sub>2</sub> on the PCE performance of the battery devices is slightly smaller, but combined with the SEM images, it can be seen that the interface modification plays a certain role in the passivation of interfacial defects to fill the surface porosity, and can also improve the overall performance of the device.

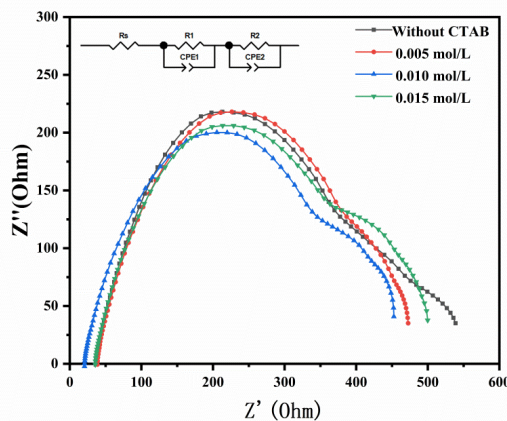


Figure 6: Electrochemical impedance of cells with TiO<sub>2</sub> as electron transport layer at different modification concentrations

To investigate the effect of CTAB gel treatment on the photogenerated electron and hole recombination behavior in perovskite solar cells, electrochemical impedance spectroscopy (EIS) measurements were performed on the devices, as shown in Figure 6. This circuit diagram has been used in other references to study carrier complexation and interfacial complexation in perovskite solar cell devices<sup>[11-13]</sup>. The equivalent circuit diagram includes a series resistor  $R_s$ , and two resistor-capacitors (RCs) to characterise the carrier transport processes in the body and at the interface, respectively. The mid- and low-frequency reflect the ion migration and the charge transfer process at the interface<sup>[14-15]</sup>.

Table 2: EIS spectrum fitting parameters of the samples with different CTAB concentrations

Samples	$R_s(\Omega)$	$R_1(\Omega)$	CPE1-T(F)	CPE1-P(F)	$R_2(\Omega)$	CPE2-T(F)	CPE2-P(F)
TiO <sub>2</sub>	3.64	9.611	$4.50 \times 10^{-4}$	0.604	24.04	0.0128	0.647
0.005	1.93	31.58	$4.95 \times 10^{-4}$	0.652	27.93	0.0180	0.602
0.010	3.44	32.23	$4.35 \times 10^{-4}$	0.664	25.83	0.0142	0.640
0.015	3.70	34.37	$4.21 \times 10^{-4}$	0.661	20.92	0.0183	0.607

The results of EIS fitting data can more intuitively see the internal effects of different doping concentrations on the device, as shown in Table 2, compared with the unmodified device, but the modification concentration of 0.005 mol/L,  $R_1$  decreased from the original 3.64  $\Omega$  to 1.93  $\Omega$ , and the transmission resistance was lowered, and with the increase of the modification concentration of 0.010 mol/L and 0.015 mol/L,  $R_1$  was close to that of the modified device, respectively 3.44  $\Omega$  and 3.70  $\Omega$ . The difference in the compound resistance of the overall device was smaller, but the modification concentration of 0.005 mol/L, its compound resistance was 27.70  $\Omega$ . The overall device had a smaller difference in compound resistance. Devices,  $R_1$  was close to that of the modified devices, which were 3.44  $\Omega$  and 3.70  $\Omega$ . The difference in composite resistance of the overall devices was small, but the composite resistance of the modified devices was 27.93  $\Omega$  at a modification concentration of 0.005 mol/L, while the composite resistance of the unmodified devices was 24.04  $\Omega$ , which was an increase in the composite resistance, indicating that the smaller modification concentration could reduce the carrier composite. The smaller transmission resistance and larger compound resistance work together to over enhance the performance of the device. Because of the smaller composite impedance of the device, more electron-hole complexes are generated and the charge complexation rate is larger, which reduces the efficiency of the device<sup>[16]</sup>.

#### 4. Conclusions

The effects of different concentrations of CTAB on the photovoltaic properties of TiO<sub>2</sub>-based PSCs were investigated by doping the TiO<sub>2</sub> films with surfactant CTAB. The films were characterized by SEM, transmittance and wetting angle. The results show that the interfacial modification of TiO<sub>2</sub> with different concentrations of CTAB can effectively disperse on the surface of TiO<sub>2</sub> film and fill the pores. When the concentration of CTAB was 0.005 mol/L, the quality of the resulting films was better with fewer pores. Appropriate increase in the roughness of the film is conducive to the spreading of the perovskite layer, at this time, the FF is 62.31%,  $J_{SC}$  is 2.88 mA/cm<sup>2</sup>,  $V_{OC}$  is 0.35 V. The EIS test results show that, when the concentration of 0.005 mol/L, the composite resistance of the device is most conducive to the efficiency of the device, the smallest transmission resistance is more conducive to the charge transfer, the largest composite resistance, can more effectively suppress the electron nulling. The maximum complex resistance is more favorable for charge transfer, and the maximum complex resistance is more effective in suppressing electron-hole complexation.

#### References

- [1] Katherine J S, Martin E B, Richard E F, et al.  $N_2O$  flux from plantsystems in polar deserts switch between sources and sinks under different light condition[J]. *Soil Biology and Biochemistry*, 2012, (48) : 69-77.
- [2] Li Mengli, Yang Xiaolong, Tang Liping, et al. Catalytic decomposition of  $N_2O$ [J]. *Advances in Chemistry*, 2012, 9: 1801-1817.
- [3] Montzka S A, Dlugokencky E J, Butler J H. Non-CO<sub>2</sub> greenhousegases and climate change[J]. *Nature*, 2011, 476(7358): 43-50.
- [4] Yi C, Luo J, Meloni S, et al. Entropic stabilization of mixed A-cation ABX<sub>3</sub> metal halide perovskites for high performance perovskite solar cells [J]. *Energy & Environmental Science*, 2016, 9(2):656-662.
- [5] Hao Huang, Peng Cui, Yan Chen et al. 24.8%-efficient planar perovskite solar cells via ligand-engineered TiO<sub>2</sub> deposition[J]. *Joule*, 2022, 6(4), 2186-2202.

- [6] H. Zhang, J. Shi, X.Xu, L. Zhu, Y. Luo, D. Li, Q. Meng. Mg-doped TiO<sub>2</sub> boosts the efficiency of planar perovskite solar cells to exceed 19% [J]. *Journal of Materials Chemistry A*. 2016, 4:15383-15389.
- [7] L. Zuo, Z. Gu, T. Ye, W. Fu, G. Wu, H. Li, H. Chen. Enhanced photovoltaic performance of CH<sub>3</sub>NH<sub>3</sub>PbI<sub>3</sub> perovskite solar cells through interfacial engineering using self-assembling monolayer [J]. *Journal of the American Chemical Society*. 2015, 137:2674-2679.
- [8] Wang C, Zhao D, Grice C R, et al. Low-temperature plasma-enhanced atomic layer deposition of tin oxide electron selective layers for highly efficient planar perovskite solar cells [J]. *Journal of Materials Chemistry A*, 2016, 4(31): 12080-12087.
- [9] Chen J, Zhao X, Kim S G, et al. Multifunctional chemical linker imidazoleacetic acid hydrochloride for 21% efficient and stable planar perovskite solar cells [J]. *Advanced Materials*, 2019, 31(39): 1902902.
- [10] Dixit S G, Mahadeshwar A R, Haram S K. Some aspects of the role of surfactants in the formation of nanoparticles [J]. *Colloids and Surfaces A: Physicochemical and Engineering Aspects*, 1998, 133(1): 69-75.
- [11] Masuko K, Shigematsu M, Hashiguchi T, et al. Achievement of More Than 25% Conversion Efficiency With Crystalline Silicon Heterojunction Solar Cell [J]. *IEEE Journal of Photovoltaics*, 2014, 4(6): 1433-1435.
- [12] Smith D D, Reich G, Baldrias M, et al. Silicon solar cells with total area efficiency above 25 % [C]; proceedings of the 2016 IEEE 43rd Photovoltaic Specialists Conference (PVSC), F 5-10 June 2016.
- [13] Tran V H, Ambade R B, Ambade S B, et al. Low-temperature solution-processed SnO<sub>2</sub> nanoparticles as cathode buffer layer for inverted organic solar cells [J]. *ACS Applied Materials & Interfaces*, 2017, 9(2): 1645-1653.
- [14] Ren X, Yang D, Yang Z, et al. Solution-processed Nb: SnO<sub>2</sub> electron transport layer for efficient planar perovskite solar cells [J]. *ACS Applied Materials & Interfaces*, 2017, 9(3): 2421-2429.
- [15] Jeon N J, Na H, Jung E H, et al. A fluorene-terminated hole-transporting material for highly efficient and stable perovskite solar cells [J]. *Nature Energy*, 2018, 3: 682-689.
- [16] Wang Yanxiang, Gao Peiyang, Fan Xueyun, etc. Effect of Interface Modification on the Performances of SnO<sub>2</sub>-based Perovskite Solar Cells [J]. *Journal of Ceramics*. 2020, 41(4): 500-506.